$(Hf_{0.25}Zr_{0.25}W_{0.25}Ti_{0.25})B_2$高熵陶瓷的组织结构与力学性能

张泽熙　张　岩　郭伟明　许　亮　张　威

（广东工业大学，广州　510006）

文　摘　为了提高高熵硼化物陶瓷的性能，扩大高熵硼化物陶瓷家族，本文通过硼热/碳热还原法结合SPS制备$(Hf_{0.25}Zr_{0.25}W_{0.25}Ti_{0.25})B_2$高熵硼化物粉末与陶瓷，并对其物相组成、组织形貌和力学性能进行研究。结果表明，经1 600 ℃热处理后$(Hf_{0.25}Zr_{0.25}W_{0.25}Ti_{0.25})B_2$高熵硼化物粉末除了检测出高熵相，还检测到$W_2B_5$第二相，粉末粒径为(0.29±0.03) μm；2 000 ℃烧结后W_2B_5减少，高熵相的衍射峰向高角度偏移，致密度达95.7%，引入WB_2后其具有优异的力学性能，硬度(21.3±1.5) GPa，断裂韧性(3.00±0.22) MPa·$m^{1/2}$。

关键词　硼热/碳热还原法，高熵硼化物，组织结构，力学性能

中图分类号：TG148　　DOI：10.12044/j.issn.1007-2330.2023.06.009

Microstructure and Mechanical Properties of $(Hf_{0.25}Zr_{0.25}W_{0.25}Ti_{0.25})B_2$ High Entropy Ceramics

ZHANG Zexi　ZHANG Yan　GUO Weiming　XU Liang　ZHANG Wei

（Guangdong University of Technology，Guangzhou　510006）

Abstract　High entropy boride ceramics have broad application prospects in aerospace, automotive engine and nuclear reactor fields. In order to improve the performance of high entropy boride ceramics and expand the family of high entropy boride ceramics, $(Hf_{0.25}Zr_{0.25}W_{0.25}Ti_{0.25})B_2$ high entropy boride ceramic was prepared by boron/carbothermal reduction combined with SPS(Spark Plasma Sintering) in this paper. The phase composition, microstructure and mechanical properties of the powder and ceramic were studied. The results show that after heat treatment at 1600℃, not only the high entropy phase but also W_2B_5 phase can be detected in $(Hf_{0.25}Zr_{0.25}W_{0.25}Ti_{0.25})B_2$ high entropy boride powder(particle size(0.29+0.03)μm). After sintering at 2000℃, the second phase W_2B_5 decreases, and the diffraction peaks of the high entropy phase shift to a higher angle. The density of ceramic reaches 95.7%. After the introduction of WB_2, the high entropy boride ceramics exhibit excellent mechanical properties. The hardness is (21.3+1.5)GPa and fracture toughness is (3.00+0.22)MPa·$m^{1/2}$.

Key words　Boro/carbothermal reduction method,High entropy borides,Microstructure,Mechanical properties

0　引言

硼化物陶瓷具有高熔点、高硬度、抗氧化和抗热震等优异性能，广泛应用于在航空航天、汽车发动机和核反应堆等领域[1-5]。近年来兴起了关于高熵硼化物陶瓷的研究，由于高熵效应，其硬度、抗氧化性和化学稳定性等得到了进一步的提升[6-8]。2016年J. GILD等[9]报道的7种高熵硼化物陶瓷的致密度约93%，但是其硬度和抗氧化性都比单一的二元硼化物高。Y. ZHANG等[10]和J. f. GU等[11]借鉴二元硼化物的合成方法，采用硼热还原法和硼热碳热还原法，原位合成高熵陶瓷粉末，粉末粒径小纯度高，其制备的高熵硼化物陶瓷的致密度>95%，硬度得到了很大的提升。研究表明，制备高熵陶瓷是提高硼化物陶瓷性能的一种途径，且获得致密的材料有利于其性能的改善。

据文献[12-13]报道，固溶不同元素也可以改变硼化物陶瓷的显微组织和力学性能。在铪基三元硼化物中，固溶TaB_2可以有效降低粉末粒径，细化陶瓷的组织结构，而掺杂TiB_2的陶瓷具有更好的力学性能[14]。二元硼化物中，WB_2(25.5 GPa)[15]具有较高的

收稿日期：2021-07-21

基金项目：国家自然科学基金(52072077，51832002)；广东省珠江人才计划地方创新团队项目(2017BT01C169)。

第一作者简介：张泽熙，1999年出生，本科，主要从事陶瓷材料研究工作。E-mail：2903576821@qq.com。

硬度。WB_2热力学不稳定，难以合成[16-17]，但是其可以与TiB_2和CrB_2等硼化物形成稳定的固溶体(TiB_2-WB_2和TiB_2-CrB_2-WB_2)[18-20]，且具有较高的硬度(>20 GPa)。M. D. QIN等[13]通过反应SPS制备的$(Hf_{0.2}Zr_{0.2}Mo_{0.2}W_{0.2}Ti_{0.25})B_2$高熵陶瓷的致密度达到97.5%，硬度26.0 GPa。但是关于含有W的四元高熵硼化物陶瓷还鲜有报道。

为了提高高熵硼化物陶瓷的性能，扩大高熵硼化物陶瓷家族，本文在铪基三元硼化物中引入WB_2，通过硼热/碳热还原法与SPS结合制备$(Hf_{0.25}Zr_{0.25}W_{0.25}Ti_{0.25})B_2$新型四元高熵硼化物陶瓷，研究其物相组成、显微结构和力学性能。

1 实验

1.1 材料

实验采用HfO_2粉(平均粒径：0.3 μm，纯度99.9%，北京泛德辰科技有限公司)、ZrO_2粉(平均粒径：0.6 μm，纯度99.8%，长沙西丽纳米研磨科技有限公司)、TiO_2粉(平均粒径：21 nm，纯度99.9%，宣城晶瑞新材料有限公司)、WO_3粉末(平均粒径：~1.0 μm，纯度99.9%，上海巷田纳米材料有限公司)、B_4C(平均粒径：1.5 μm，纯度99.9%，牡丹江金刚钻碳化硼有限公司)和C粉(平均粒径：2.0 μm，纯度99.9%，上海胶体化工有限公司)为原料。

1.2 试验方法

按照目标产物为$(Hf_{0.25}Zr_{0.25}W_{0.25}Ti_{0.25})B_2$，将原料粉末称量，为了弥补在硼热/碳热还原反应过程中硼源的损失，B_4C粉过量27 wt%，并相应的减少C粉的含量，以球料比2∶1，在聚乙烯瓶子中采用乙醇和Si_3N_4球磨介质，球磨24 h后旋转蒸发干燥。之后将混合粉末过75 μm，压入模具中(直径约30 mm，厚度为5 mm)，然后将混合粉末置于真空无压炉中(LHS-2，中山凯旋真空技术工程有限公司)，为了给硼热/碳热反应提供足够的反应驱动力，在真空气氛下，以10 ℃/min的升温速率升温到1600 ℃，保温1 h后合成出高熵硼化物粉末。之后将高熵硼化物粉末研磨过100目筛后，装入石墨模具中，以150 ℃/min升温速率升温到2 000 ℃保温5 min，加压30 MPa，在氩气气氛下放电等离子(H-HPD10-FL，FCT SystemeGmbh)烧结制备高熵硼化物陶瓷。烧结后的试样经过表面打磨、仔细抛光后放在无水乙醇中超声波清洗10 min，然后取出试样干燥。

1.3 测试仪器及方法

材料相对密度用阿基米德法测量(TG-328A型光电分析天平)。在德国Bruker公司D8 ADVANCE X射线衍射仪上对本实验的高熵硼化物粉末和陶瓷块体进行物相分析。采用Cu-Kα辐射，镍片滤液，陶瓷X光管功率为3 kW，粉末的XRD分析的步进为0.0263°，陶瓷块体的XRD分析的步进为0.0131°。在Nova NanoSEM430扫描电子显微镜上结合能量色散光谱(EDS；X-MarN，Oxford)对高熵硼化物粉末形貌、高熵硼化物陶瓷的组织结构、元素分布和断口形貌进行观察研究。

用GB/T16534—96在HVS-30Z型维氏硬度计上测试材料的维氏硬度，每个试样至少10个点，载荷为1.96 N，保压时间为15 s。室温断裂韧性由压痕法测出[21]，载荷98 N，保压时间10 s。

2 实验结果与讨论

2.1 合成粉体分析

根据硼热/碳热还原法制备HfB_2粉末的反应[22]，HfO_2首先与B_4C反应生成HfB_2和B_2O_3：

$$HfO_2 + \frac{5}{7}B_4C = HfB_2 + \frac{3}{7}B_2O_3 + \frac{5}{7}CO(g) \quad (1)$$

然后，HfO_2、B_2O_3和C继续反应生成HfB_2：

$$HfO_2 + B_2O_3 + 5C = HfB_2 + 5CO(g) \quad (2)$$

类似，在高熵陶瓷粉体合成过程中，氧化物首先与B_4C反应生成高熵硼化物和B_2O_3：

$$HfO_2 + ZrO_2 + WO_3 + TiO_2 + 3B_4C = 4(Hf_{0.25}Zr_{0.25}W_{0.25}Ti_{0.25})B_2 + 3CO(g) + 2B_2O_3 \quad (3)$$

然后氧化物继续和B_2O_3、C反应生成高熵硼化物：

$$HfO_2 + ZrO_2 + WO_3 + TiO_2 + 4B_2O_3 + 21C = 4(Hf_{0.25}Zr_{0.25}W_{0.25}Ti_{0.25})B_2 + 21CO(g) \quad (4)$$

由于B_2O_3具有高的蒸气压，在低于1 450℃就会挥发，因此会造成反应过程中B源的减少，剩余的氧化物和C会发生如下的反应生成碳化物杂质：

$$HfO_2 + ZrO_2 + WO_3 + TiO_2 + 13C = 4(Hf_{0.25}Zr_{0.25}W_{0.25}Ti_{0.25})C + 9CO(g) \quad (5)$$

因此在硼热/碳热还原反应的过程中需要加入过量的B_4C来弥补硼源的损失，而B_4C增加会同时增加B的含量和C的含量，所以要相应减少C粉的含量，防止其与氧化物生成碳化物杂质。

我们对其氧化物各自的反应方程式进行热力学计算发现，温度高于1 450 ℃时所有的反应均能发生，如图1所示。为了让B_2O_3尽可能挥发完全，本文选择1 600 ℃作为反应温度。

图2(a)是$(Hf_{0.25}Zr_{0.25}W_{0.25}Ti_{0.25})B_2$高熵硼化物粉末和陶瓷的XRD图谱。可见，原料粉末经1 600 ℃/1 h反应之后，除了相应的主要高熵相之外，在$(Hf_{0.25}Zr_{0.25}W_{0.25}Ti_{0.25})B_2$高熵硼化物粉末中检测出大量的$W_2B_5$相；但是在$(Hf_{0.25}Zr_{0.25}W_{0.25}Ti_{0.25})B_2$高熵粉末中均未检测出氧化物杂质相，如图2(a)曲线①所

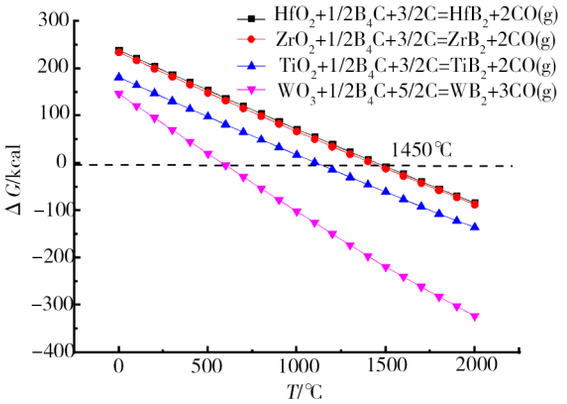

图1　HfO_2、ZrO_2、WO_3和TiO_2硼热/碳热反应中ΔG随温度的变化曲线

Fig. 1　ΔG with temperature curve in boron/carbonthermal reaction of HfO_2, ZrO_2, WO_3 and TiO_2

示，这表明在1 600 ℃时，硼热/碳热还原反应进行完全，没有氧化物杂质剩余。

2.1　烧结陶瓷分析

经2 000 ℃放电等离子烧结后，从$(Hf_{0.25}Zr_{0.25}W_{0.25}Ti_{0.25})B_2$的33°~45°的放大XRD图谱中可以看出，高温烧结后仍含有W_2B_5，如图2(b)曲线②所示。大部分的W_2B_5相固溶进高熵相中，高熵相的衍射峰向高角度偏移，如图2(b)所示。通过Jade软件精修计算出$(Hf_{0.25}Zr_{0.25}W_{0.25}Ti_{0.25})B_2$晶格常数为$a$=0.309 99 nm，$c$=0.33801 nm。$(Hf_{0.25}Zr_{0.25}W_{0.25}Ti_{0.25})B_2$高熵相含量为97.3wt%，$W_2B_5$第二相为2.7wt%。

图3是$(Hf_{0.25}Zr_{0.25}W_{0.25}Ti_{0.25})B_2$高熵硼化物粉末的SEM照片，从图中可以看出粉末形状为类球形，且大小分布均匀。$(Hf_{0.25}Zr_{0.25}W_{0.25}Ti_{0.25})B_2$的晶粒尺寸为(0.29±0.03) μm，通过硼热/碳热还原法合成的高熵陶瓷粉末均较细，如表1所示。之前报道，在相同原料和相同工艺的前提下，通过硼热/碳热还原反应制备的HfB_2和ZrB_2较粗(2~3 μm)，这是由于在反应过程中存在B_2O_3副产物，其蒸发凝聚作用使得硼化物粉末粗化[22-23]。GUO等通过在HfB_2和ZrB_2固溶TiB_2或者Ta_2B_5有效的抑制了B_2O_3蒸发凝聚作用，降低了粉末粒径(0.2~1.0 μm)[14]，在本研究中，以等摩尔比原位引入4种硼化物形成高熵硼化物固溶体，多种元素固溶进一步抑制了B_2O_3蒸发凝聚作用，细化粉末粒径。

根据XRD定量计算得知$(Hf_{0.25}Zr_{0.25}W_{0.25}Ti_{0.25})B_2$高熵硼化物陶瓷的理论密度为8.51 g/cm^3。$(Hf_{0.25}Zr_{0.25}W_{0.25}Ti_{0.25})B_2$高熵硼化物陶瓷的致密度为(95.7±0.3)%，如表1所示。

图4(a)是$(Hf_{0.25}Zr_{0.25}W_{0.25}Ti_{0.25})B_2$高熵硼化物陶瓷的断口形貌，可以看出，$(Hf_{0.25}Zr_{0.25}W_{0.25}Ti_{0.25})B_2$高

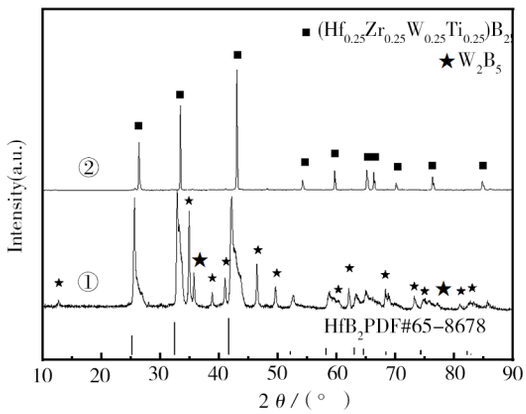

(a)　$(Hf_{0.25}Zr_{0.25}W_{0.25}Ti_{0.25})B_2$ 高熵陶瓷

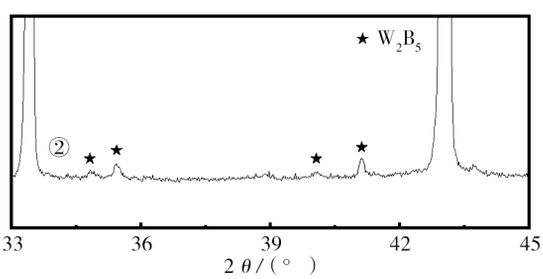

(b)　曲线②局部放大

图2　$(Hf_{0.25}Zr_{0.25}W_{0.25}Ti_{0.25})B_2$高熵陶瓷的XRD图谱

Fig. 2　XRD pattern of $(Hf_{0.25}Zr_{0.25}W_{0.25}Ti_{0.25})B_2$ high-entropy boride

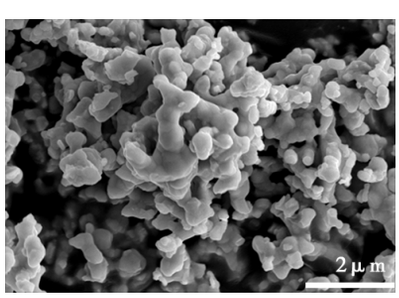

图3　$(Hf_{0.25}Zr_{0.25}W_{0.25}Ti_{0.25})B_2$高熵陶瓷粉末的SEM照片

Fig. 3　SEM images of $(Hf_{0.25}Zr_{0.25}W_{0.25}Ti_{0.25})B_2$ high-entropy boride powder

表1　$(Hf_{0.25}Zr_{0.25}W_{0.25}Ti_{0.25})B_2$性能参数

Tab. 1　Performance parameters of $(Hf_{0.25}Zr_{0.25}W_{0.25}Ti_{0.25})B_2$

粉末粒径/μm	晶粒尺寸/μm	相对密度/%	硬度/GPa	断裂韧性/MPa·m$^{1/2}$
0.29±0.03	2.39±0.92	95.7±0.3	21.3±1.5	3.00±0.22

熵硼化物陶瓷中观察到了很多气孔，与致密度测试结果一致。在$(Hf_{0.25}Zr_{0.25}W_{0.25}Ti_{0.25})B_2$样品中还观察到大量白色小颗粒，从XRD结果推测其为W_2B_5第二相。$(Hf_{0.25}Zr_{0.25}W_{0.25}Ti_{0.25})B_2$的断裂方式为穿晶断裂。图4(b)是$(Hf_{0.25}Zr_{0.25}W_{0.25}Ti_{0.25})B_2$高熵硼化物陶瓷抛光面腐蚀后的形貌。$(Hf_{0.25}Zr_{0.25}W_{0.25}Ti_{0.25})B_2$的晶粒尺寸为(2.39±0.92) μm，由于自合成的高熵陶瓷粉末较细，烧结后的晶粒尺寸也较小。

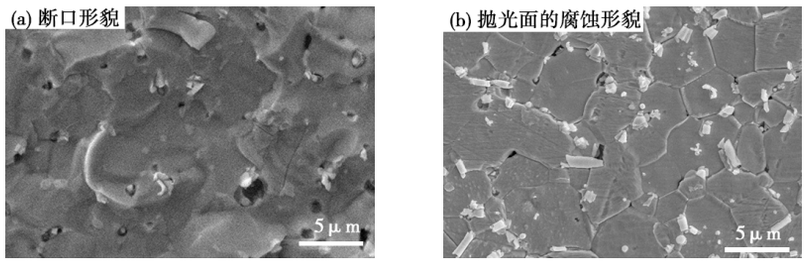

图4 $(Hf_{0.25}Zr_{0.25}W_{0.25}Ti_{0.25})B_2$高熵硼化物陶瓷的腐蚀形貌

Fig. 4 Corrosion morphology of $(Hf_{0.25}Zr_{0.25}W_{0.25}Ti_{0.25})B_2$ high-entropy boride ceramic

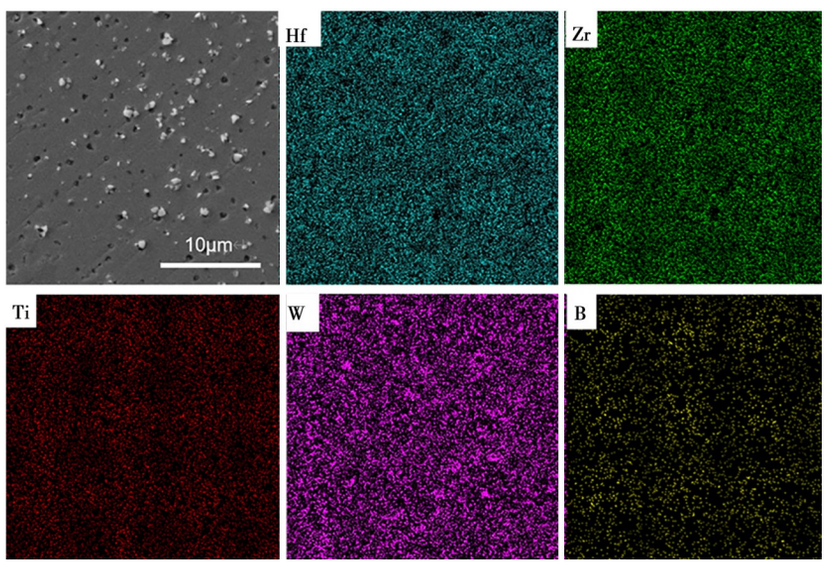

图5 $(Hf_{0.25}Zr_{0.25}W_{0.25}Ti_{0.25})B_2$高熵陶瓷的面扫描分布图

Fig. 5 EDS mapping of $(Hf_{0.25}Zr_{0.25}W_{0.25}Ti_{0.25})B_2$ high-entropy boride ceramic

为了确定$(Hf_{0.25}Zr_{0.25}W_{0.25}Ti_{0.25})B_2$高熵硼化物陶瓷的元素分布，对其进行面扫描分析。从图5中可以看出$(Hf_{0.25}Zr_{0.25}W_{0.25}Ti_{0.25})B_2$样品中有灰色相和白色相，除了W元素，其他元素均分布均匀，白色相中W元素出现了聚集，证明白色相富含W，与XRD测试结果一致。由于白色相较小，无法进行点扫描分析，从XRD结果推测其为W_2B_5第二相。

$(Hf_{0.25}Zr_{0.25}W_{0.25}Ti_{0.25})B_2$的硬度和断裂韧性分别为(21.3±1.5) GPa 和(3.00±0.22) MPa·$m^{1/2}$。由于WB_2、TiB_2、ZrB_2与HfB_2的晶格常数的差异，当发生固溶时会造成晶格畸变，抑制位错和滑移，提高材料的硬度，所以$(Hf_{0.25}Zr_{0.25}W_{0.25}Ti_{0.25})B_2$高熵陶瓷的硬度较高，此外含W的硼化物的硬度较高[15]，根据混合法则，高硬度的W_2B_5第二相的存在对$(Hf_{0.25}Zr_{0.25}W_{0.25}Ti_{0.25})B_2$高熵陶瓷的硬度提高起到了一定的作用，所以$W_2B_5$第二相的$(Hf_{0.25}Zr_{0.25}W_{0.25}Ti_{0.25})B_2$高熵陶瓷的硬度较高，接近五元高熵的硬度(19~25 GPa)[9,24-25]。

由于$(Hf_{0.25}Zr_{0.25}W_{0.25}Ti_{0.25})B_2$样品中存在的$W_2B_5$第二相颗粒尺寸小，且均匀分布晶界和三角汇集处，在裂纹扩展时，延长裂纹扩展路径，提高其断裂韧性[26]。从$(Hf_{0.25}Zr_{0.25}W_{0.25}Ti_{0.25})B_2$高熵陶瓷的裂纹扩展照片可看出其裂纹扩展路径较为弯曲，其在W_2B_5第二相位置处有一定的偏转，如图6白色箭头所示，因此$(Hf_{0.25}Zr_{0.25}W_{0.25}Ti_{0.25})B_2$样品的断裂韧性较高。

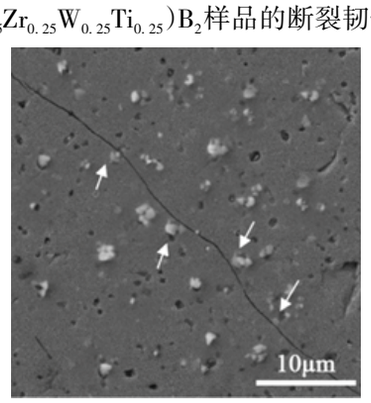

图6 $(Hf_{0.25}Zr_{0.25}W_{0.25}Ti_{0.25})B_2$高熵陶瓷的裂纹扩展照片

Fig. 6 Crack propagation photograph of $(Hf_{0.25}Zr_{0.25}W_{0.25}Ti_{0.25})B_2$ high-entropy boride ceramic

3 结论

本文通过硼热/碳热还原法结合SPS制备$(Hf_{0.25}Zr_{0.25}W_{0.25}Ti_{0.25})B_2$高熵硼化物粉末与陶瓷，并对其物相组成、组织形貌和力学性能进行研究。结果表明：

(1)固溶WB_2后，$(Hf_{0.25}Zr_{0.25}W_{0.25}Ti_{0.25})B_2$高熵硼化物粉末和陶瓷均未形成单相固溶体，除了检测出

高熵相，还检测出W_2B_5第二相；

（2）$(Hf_{0.25}Zr_{0.25}W_{0.25}Ti_{0.25})B_2$高熵硼化物的致密度~95%，晶粒尺寸较小（2.39±0.92）μm；

（3）$(Hf_{0.25}Zr_{0.25}W_{0.25}Ti_{0.25})B_2$高熵硼化物陶瓷具有优异的力学性能，硬度（21.3±1.5）GPa，断裂韧性（3.00±0.22）$MPa\cdot m^{1/2}$。

参考文献

[1] ZHANG Zhaofu, SHA Jianjun, ZU Yufei, et al. Fabrication and mechanical properties of self-toughening ZrB_2-SiC composites from in-situ reaction[J]. Journal of Advanced Ceramics, 2019, 8(4): 527-536.

[2] LIU Da, FU Qiangang, CHU Yanhui. Molten salt synthesis, formation mechanism, and oxidation behavior of nanocrystalline HfB_2 powders [J]. Journal of Advanced Ceramics, 2020, 9(1): 35-44.

[3] GOLLA B R, MUKHOPADHYAY A, BASU B, et al. Review on ultra high temperature boride ceramics[J]. Progress in Materials Science, 2020, 111: 100651.

[4] FAHRENHOLTZ W G, HILMAS G E, TALMY I G, et al, Refractory diborides of zirconium and hafnium[J]. Journal of the American Ceramic Society, 2007, 90(5): 1347-1364.

[5] 李麒，郭丰伟，曹腊梅，等. PS烧结温度对ZrB_2-SiC复合陶瓷性能的影响[J]. 空材料学报，018，38(4)：87-92.

LI Qi, GUO Fengwei, CAO Lamei, et al. Effect of SPS sintering temperature on properties of ZrB_2-SiC ceramic [J]. Journal of Aeronautical Materials, 2018, 38(4): 87-92.

[6] ZHANG Yan, GUO Weiming, JIANG Zebin, et al. Dense high-entropy boride ceramics with ultra-high hardness [J]. Scripta Materialia, 2019, 164: 135-139.

[7] GILD J, KAUFMANN K, VECCHIO K, et al. Reactive flash spark plasma sintering of high-entropy ultrahigh temperature ceramics [J]. Scripta Materialia, 2019, 170: 106-110.

[8] ZHANG Yan, JIANG Zebin, SUN Shikuan, et al. Microstructure and mechanical properties of high-entropy borides derived from boro/carbothermal reduction[J]. Journal of the European Ceramic Society, 2019, 39(13): 3920-3924.

[9] GILD J, ZHANG Yuanyao, HARRINGTON T, et al. High-entropy metal diborides: a new class of high-entropy materials and a new type of ultrahigh temperature ceramics[J]. Scientific Reports, 2016, 6: 37946.

[10] ZHANG Yan, SUN ShiKuan, ZHANG Wei, et al. Improved densification and hardness of high-entropy diboride ceramics from fine powders synthesized via borothermal reduction process[J]. Ceramic International, 2020, 46(9): 14299-14303.

[11] GU Junfeng, ZOU Ji, SUN Shikuan, et al. Dense and pure high-entropy metal diboride ceramics sintered from self-synthesized powders via boro/carbothermal reduction approach [J]. Science China Materials, 2019, 62(12): 1898-1909.

[12] GILD J, WRIGHT A, QUIAMBAO-TOMKO K, et al. Thermal conductivity and hardness of three single-phase high-entropy metal diborides fabricated by borocarbothermal reduction and spark plasma sintering[J]. Ceramic International, 2020, 46(5): 6906-6913.

[13] QIN Mingde, GILD J, WANG Haoren, et al. Dissolving and stabilizing soft WB_2 and MoB_2 phases into high-entropy borides via boron-metals reactive sintering to attain higher hardness[J]. Journal of the European Ceramic Society, 2020, 40(12): 4348-4353.

[14] ZHANG Wei, ZHANG Yan, GUO Weiming, et al. Powder synthesis, densification, microstructure and mechanical properties of Hf-based ternary boride ceramics[J]. Journal of the European Ceramic Society, 2021, 41(7): 3922-3928.

[15] WANG Changchun, SONG Lele, XIE Yupeng. Mechanical and electrical characteristics of WB_2 synthesized at high pressure and high temperature[J]. Materials, 2020, 13(5): 1212.

[16] CHEN Xingqiu, FU C L, KRČMAR M, et al. Electronic and structural origin of ultra incompressibility of 5d transition-metal diborides MB_2 (M = W, Re, Os)[J]. Physical Review Letters, 2008, 100(19): 196403.

[17] ZHAO Erjun, MENG Jian, MA Yanming, et al. Phase stability and mechanical properties of tungsten borides from first principles calculations [J]. Physical Chemistry Chemical Physics, 2010, 12(40): 13158-13165.

[18] SHIBUYA M, KAWATA M, OHYANAGI M, et al. Titanium diboride-tungsten diboride solid solutions formed by induction-field-activated combustion synthesis [J]. Journal of the American Ceramic Society, 2003, 86(4): 706-710.

[19] SHIBUYA M, YAMAMOTO Y, OHYANAGI M. Simultaneous densification and phase decomposition of TiB_2-WB_2 solid solutions activated by cobalt boride addition [J]. Journal of the European Ceramic Society, 2007, 7 1): 07-312.

[20] KAGA H, HEIAN E M, MUNIR Z A, et al. Synthesis of hard materials by field activation: the synthesis of solid solutions and composites in the TiB_2-WB_2-CrB_2 system [J]. Journal of the American Ceramic Society, 2001, 84(12): 2764-2770

[21] EVANS A G, CHARLES E A. Fracture toughness determinations by indentation [J]. Journal of the American Ceramic Society, 1976, 59: 371-372.

[22] NI Dewei, ZHANG Guojun, KAN Yanmei, et al. Synthesis of monodispersed fine hafnium diboride powders using carbo/borothermal reduction of hafnium dioxide[J]. Journal of the American Ceramic Society, 2008, 91(8): 2709-2712.

[23] GUO Weiming, ZHANG Guojun. Reaction processes and characterization of ZrB_2 powder prepared by boro/carbothermal reduction of ZrO_2 in vacuum[J]. Journal of the American Ceramic Society, 2009, 92(1): 264-267.

[24] TALLARITA G, LICHERI R, GARRONI S, et al. Novel processing route for the fabrication of bulk high-entropy metal diborides[J]. Scripta Materialia, 2019, 158: 100-104.

[25] FENG Lun, FAHRENHOLTZ W G, HILMAS G E. Processing of dense high-entropy boride ceramics[J]. Journal of the European Ceramic Society, 2020, 40(12): 3815-3823.

[26] SHEN Xiaoqin, LIU Jixuan, LI Fei, et al. Preparation and characterization of diboride-based high entropy $(Ti_{0.2}Zr_{0.2}Hf_{0.2}Nb_{0.2}Ta_{0.2})B_2$-SiC particulate composites [J]. Ceramic International, 2019, 45(18): 24508-24514.